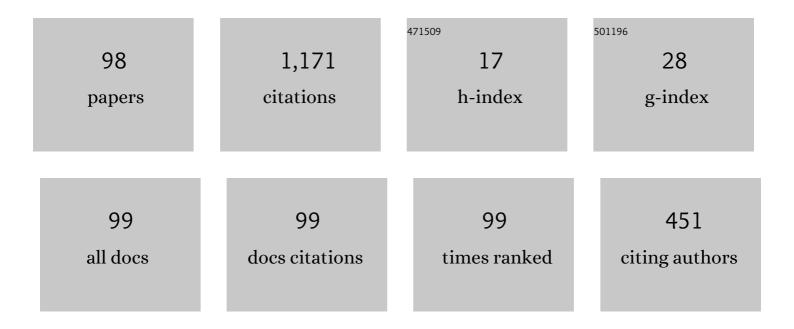
Tsuyoshi Yoshitake

List of Publications by Year in descending order

Source: https://exaly.com/author-pdf/5162619/publications.pdf Version: 2024-02-01



#	Article	IF	CITATIONS
1	Laser-induced novel ohmic contact formation for effective charge collection in diamond detectors. Materials Science in Semiconductor Processing, 2022, 139, 106370.	4.0	10
2	Monothetic Analysis and Response Surface Methodology Optimization of Calcium Alginate Microcapsules Characteristics. Polymers, 2022, 14, 709.	4.5	13
3	Evaluation of Hydrogen-Induced Blistering of Mo/Si Multilayers with a Capping Layer. Plasma and Fusion Research, 2022, 17, 1406005-1406005.	0.7	6
4	Correlated Electrical Conductivities to Chemical Configurations of Nitrogenated Nanocrystalline Diamond Films. Nanomaterials, 2022, 12, 854.	4.1	9
5	Formation of p-n ⁺ diamond homojunctions by shallow doping of phosphorus through liquid emersion excimer laser irradiation. Materials Research Letters, 2022, 10, 666-674.	8.7	6
6	Temperature-Dependent Impedance Spectra of Nitrogen-Doped Ultrananocrystalline Diamond Films Grown on Si Substrates. IEEE Access, 2021, 9, 896-904.	4.2	2
7	Effects of substrate temperature and intermediate layer on adhesion, structural and mechanical properties of coaxial arc plasma deposition grown nanodiamond composite films on Si substrates. Surface and Coatings Technology, 2021, 417, 127185.	4.8	15
8	Physical Properties of Fe3Si Films Coated through Facing Targets Sputtering after Microwave Plasma Treatment. Coatings, 2021, 11, 923.	2.6	6
9	Enhanced in-plane uniformity and breakdown strength of diamond Schottky barrier diodes fabricated on heteroepitaxial substrates. Japanese Journal of Applied Physics, 2021, 60, SBBD05.	1.5	12
10	Diamond/β-Ga2O3 pn heterojunction diodes fabricated by low-temperature direct-bonding. AIP Advances, 2021, 11, .	1.3	15
11	Diode parameters and ultraviolet light detection characteristics of n-type silicon/p-type nanocrystalline diamond heterojunctions at different temperatures. Thin Solid Films, 2020, 709, 138222.	1.8	2
12	Diode Parameters and Equivalent Electrical Circuit Model of n-Type Silicon/B-Doped p-Type Ultrananocrystalline Diamond Heterojunctions Manufactured Through Coaxial Arc Plasma Deposition. Journal of Nanoscience and Nanotechnology, 2020, 20, 4884-4891.	0.9	0
13	Impact of annealing temperature and carbon doping on the wetting and surface morphology of semiconducting iron disilicide formed via radio frequency magnetron sputtering. Thin Solid Films, 2020, 709, 138248.	1.8	7
14	Analysis of Electrical Characteristics of Pd/ <i>n</i> -Nanocarbon/ <i>p</i> -Si Heterojunction Diodes: By <i>C</i> - <i>V</i> - <i>f</i> and <i>G</i> / <i>w</i> - <i>V</i> - <i>f</i> . Journal of Nanomaterials, 2020, 2020, 1-9.	2.7	9
15	Laser-Induced Phosphorus-Doped Conductive Layer Formation on Single-Crystal Diamond Surfaces. ACS Applied Materials & Interfaces, 2020, 12, 57619-57626.	8.0	13
16	Electrochemical detection characteristics of the composite films of boronâ€doped nanocrystalline diamond and amorphous carbon prepared using the coaxial arc plasma deposition method. IEEJ Transactions on Electrical and Electronic Engineering, 2020, 15, 1121-1122.	1.4	0
17	Near- and far-field Raman spectroscopic studies of nanodiamond composite films deposited by coaxial arc plasma. Applied Physics Letters, 2020, 116, .	3.3	14
18	Impedance spectroscopy analysis of n-type (nitrogen-doped) ultrananocrystalline diamond/p-type Si heterojunction diodes. Physica Scripta, 2020, 95, 095803.	2.5	9

#	Article	IF	CITATIONS
19	Influence of Annealing Temperature on Mechanical and Wetting Properties of <i>^î²</i> -FeSi ₂ Films Built Using Facing-Targets Direct-Current Sputtering. Journal of Nanoscience and Nanotechnology, 2020, 20, 621-628.	0.9	5
20	Wettability, Surface Morphology and Structural Properties of β-FeSi2 Films Manufactured Through Usage of Radio-Frequency Magnetron Sputtering. Journal of Nanoscience and Nanotechnology, 2020, 20, 5075-5081.	0.9	1
21	Structural evolution of laser-irradiated ultrananocrystalline diamond/amorphous carbon composite films prepared by coaxial arc plasma. Applied Physics Express, 2020, 13, 105503.	2.4	17
22	Light Detection and Carrier Transportation Mechanism in p-Type Si/n-Type Nanocrystalline FeSi2 Heterojunctions Produced via Radio-Frequency Magnetron Sputtering. Journal of Nanoscience and Nanotechnology, 2020, 20, 5082-5088.	0.9	1
23	Extraction of <i>J</i> – <i>V</i> , <i>G/ï‰</i> 〓 <i>V</i> – <i>V</i> A– <i>V</i> A– <i>V</i> Aâ€	0.9	0
24	Temperature Dependence of Alternating Current Impedance in n-Type Si/B-Doped p-Type Ultrananocrystalline Diamond Heterojunctions Produced Through Pulsed Laser Deposition. Journal of Nanoscience and Nanotechnology, 2020, 20, 331-337.	0.9	0
25	Laser-induced structure transition of diamond-like carbon coated on cemented carbide and formation of reduced graphene oxide. MRS Communications, 2019, 9, 910-915.	1.8	12
26	Effect of Annealing on Surface Morphology and Wettability of NC-FeSi ₂ Films Produced via Facing-Target Direct-Current Sputtering. Journal of Nanoscience and Nanotechnology, 2019, 19, 6834-6840.	0.9	6
27	Enhanced hardness of nanocarbon films deposited on cemented tungsten carbide substrates by coaxial arc plasma deposition owing to employing silicon-doped graphite targets. Japanese Journal of Applied Physics, 2019, 58, 075507.	1.5	6
28	C–V–f, G–V–f and Z″–Z′ Characteristics of n-Type Si/B-Doped p-Type Ultrananocrystalline Diamo Heterojunctions Formed via Pulsed Laser Deposition. Journal of Nanoscience and Nanotechnology, 2019, 19, 6812-6820.	ond 0.9	4
29	Negative bias effects on deposition and mechanical properties of ultrananocrystalline diamond/amorphous carbon composite films deposited on cemented carbide substrates by coaxial arc plasma. Diamond and Related Materials, 2019, 96, 67-73.	3.9	12
30	Electrical properties of boron-incorporated ultrananocrystalline diamond/hydrogenated amorphous carbon composite films. Applied Physics A: Materials Science and Processing, 2019, 125, 1.	2.3	4
31	Formation of low resistivity layers on singlecrystalline diamond by excimer laser irradiation. Diamond and Related Materials, 2019, 95, 166-173.	3.9	12
32	Optical and structural characterization of ultrananocrystalline diamond/hydrogenated amorphous carbon composite films deposited via coaxial arc plasma. Current Applied Physics, 2019, 19, 143-148.	2.4	13
33	Diode Parameters of Heterojunctions Comprising p-Type Ultrananocrystalline Diamond Films and n-Type Si Substrates. Journal of Nanoscience and Nanotechnology, 2019, 19, 1567-1573.	0.9	4
34	Photovoltaic Properties and Series Resistance of p-Type Si/Intrinsic Si/n-Type Nanocrystalline FeSi2 Heterojunctions Created by Utilizing Facing-Targets Direct-Current Sputtering. Journal of Nanoscience and Nanotechnology, 2019, 19, 1445-1450.	0.9	4
35	Minority carrier lifetime in ultrananocrystalline diamond/hydrogenated amorphous carbon composite films. Transactions of the Materials Research Society of Japan, 2018, 43, 361-364.	0.2	3
36	Effects of Air Exposure on Hard and Soft X-ray Photoemission Spectra of Ultrananocrystalline Diamond/Amorphous Carbon Composite Films. Coatings, 2018, 8, 359.	2.6	5

#	Article	IF	CITATIONS
37	Production of pâ€Type Si/nâ€Type βâ€FeSi ₂ Heterojunctions Using Facingâ€Targets Directâ€Currer Sputtering and Evaluation of Their Resistance and Interface State Density. Physica Status Solidi (A) Applications and Materials Science, 2018, 215, 1701022.	nt 1.8	7
38	Minority carrier lifetime in ultrananocrystalline diamond/hydrogenated amorphous carbon composite films. Transactions of the Materials Research Society of Japan, 2018, 43, 49-52.	0.2	1
39	Pulsed laser irradiation as a process of conductive surface formation on nanopolycrystalline diamond. Japanese Journal of Applied Physics, 2018, 57, 118004.	1.5	1
40	Characterization and design optimization of heterojunction photodiodes comprising n-type ultrananocrystalline diamond/hydrogenated amorphous carbon composite and p-type Si. Materials Science in Semiconductor Processing, 2018, 86, 115-121.	4.0	13
41	Effects of hydrogenation on thermal conductivity of ultrananocrystalline diamond/amorphous carbon composite films prepared via coaxial arc plasma deposition. Applied Physics Express, 2018, 11, 065101.	2.4	2
42	Thermal Conductivity of Ultrananocrystalline Diamond/Hydrogenated Amorphous Carbon Composite Films Prepared by Coaxial Arc Plasma Deposition. ECS Transactions, 2017, 75, 27-32.	0.5	3
43	Interface-state density estimation of n-type nanocrystalline FeSi 2 /p-type Si heterojunctions fabricated by pulsed laser deposition. Advances in Natural Sciences: Nanoscience and Nanotechnology, 2017, 8, 035016.	1.5	1
44	Temperature-dependent current–voltage characteristics and ultraviolet light detection of heterojunction diodes comprising n-type ultrananocrystalline diamond/hydrogenated amorphous carbon composite films and p-type silicon substrates. Japanese Journal of Applied Physics, 2017, 56, 07KD04.	1.5	11
45	Application of nitrogen-doped ultrananocrystalline diamond/hydrogenated amorphous carbon composite films for ultraviolet detection. Applied Physics A: Materials Science and Processing, 2017, 123, 1.	2.3	21
46	Fabrication of Nanocomposite AlN Hard Coating Film by Reactive Coaxial Arc Plasma Deposition. Hyomen Gijutsu/Journal of the Surface Finishing Society of Japan, 2017, 68, 735-737.	0.2	0
47	Low-temperature carrier transport properties of n-type ultrananocrystalline diamond/p-type Si heterojunction diodes. , 2016, , .		1
48	Evaluation of photovoltaic properties of nanocrystalline-FeSi 2 /Si heterojunctions. Solid-State Electronics, 2016, 123, 111-118.	1.4	9
49	Hard coating of ultrananocrystalline diamond/nonhydrogenated amorphous carbon composite films on cemented tungsten carbide by coaxial arc plasma deposition. Applied Physics A: Materials Science and Processing, 2016, 122, 1.	2.3	20
50	Effects of nitrogen doping on the electrical conductivity and optical absorption of ultrananocrystalline diamond/hydrogenated amorphous carbon films prepared by coaxial arc plasma deposition. Japanese Journal of Applied Physics, 2016, 55, 07LE01.	1.5	11
51	Room-temperature hard coating of ultrananocrystalline diamond/nonhydrogenated amorphous carbon composite films on tungsten carbide by coaxial arc plasma deposition. Japanese Journal of Applied Physics, 2016, 55, 030302.	1.5	9
52	Synthesis method for ultrananocrystalline diamond in powder employing a coaxial arc plasma gun. Applied Physics Express, 2015, 8, 075101.	2.4	10
53	Hydrogenation effects on carrier transport in boron-doped ultrananocrystalline diamond/amorphous carbon films prepared by coaxial arc plasma deposition. Journal of Vacuum Science and Technology A: Vacuum, Surfaces and Films, 2015, 33, 061514.	2.1	15
54	Near-Edge X-ray Absorption Fine-Structure Study on Hydrogenated Boron-Doped Ultrananocrystalline Diamond/Amorphous Carbon Composite Films Prepared by Coaxial Arc Plasma Deposition. Transactions of the Materials Research Society of Japan, 2015, 40, 243-246.	0.2	5

#	Article	IF	CITATIONS
55	Hardness and modulus of ultrananocrystalline diamond/hydrogenated amorphous carbon composite films prepared by coaxial arc plasma deposition. Applied Physics A: Materials Science and Processing, 2015, 119, 205-210.	2.3	7
56	Influences of repetition rate of arc discharges on hardness and modulus of ultrananocrystalline diamond films prepared by coaxial arc plasma deposition. Materials Research Express, 2015, 2, 015021.	1.6	0
57	Electrical characteristics of nitrogen-doped ultrananocrystalline diamond/hydrogenated amorphous carbon composite films prepared by coaxial arc plasma deposition. Applied Physics Express, 2015, 8, 095101.	2.4	26
58	Carrier transport and photodetection in heterojunction photodiodes comprising n-type silicon and p-type ultrananocrystalline diamond/hydrogenated amorphous carbon composite films. Japanese Journal of Applied Physics, 2014, 53, 050307.	1.5	10
59	Temperatureâ€dependent interlayer coupling in Fe ₃ <scp>S</scp> i/scp>Fe <scp>S</scp> i ₂ artificial lattices. Physica Status Solidi (A) Applications and Materials Science, 2014, 211, 323-328.	1.8	6
60	Chemical Bonding of Nitrogenated Ultrananocrystalline Diamond Films Deposited on Titanium Substrates by Pulsed Laser Deposition. ECS Journal of Solid State Science and Technology, 2013, 2, M33-M38.	1.8	2
61	Near-infrared photodetection of β-FeSi2/Si heterojunction photodiodes at low temperatures. Applied Physics Letters, 2013, 102, .	3.3	38
62	Fabrication of mesa structural n-type nanocrystalline-FeSi2/p-type Si heterojunction photodiodes by liftoff technique combined with photolithography. Physica Status Solidi C: Current Topics in Solid State Physics, 2013, 10, 1785-1788.	0.8	9
63	Magnetoresistance effects in currentâ€perpendicularâ€toâ€plane structures based on Fe ₃ Si/FeSi ₂ artificial lattices. Physica Status Solidi C: Current Topics in Solid State Physics, 2013, 10, 1862-1865.	0.8	5
64	Influences of hydrogen passivation on NIR photodetection of n-type Î ² -FeSi2/p-type Si heterojunction photodiodes fabricated by facing-targets direct-current sputtering. Materials Research Society Symposia Proceedings, 2012, 1396, .	0.1	1
65	Roles of boron in growth of diamond grains in ultrananocrystalline diamond/hydrogenated amorphous carbon composite films prepared by pulsed laser deposition. Materials Research Society Symposia Proceedings, 2012, 1395, 69.	0.1	0
66	Deep-Ultraviolet Light Detection of p-Type Ultrananocrystalline Diamond/Hydrogenated Amorphous Carbon Composite Films. Applied Physics Express, 2012, 5, 065202.	2.4	27
67	Preparation of Diamond Nanocrystallites in Powder by Using a Coaxial Arc Plasma Gun. Materials Research Society Symposia Proceedings, 2012, 1395, 99.	0.1	Ο
68	Interface Properties of Nanocrystalline-\${m FeSi}_{2}\$/Crystalline-Si Near-Infrared Heterojunction Photodiodes. IEEE Journal of Quantum Electronics, 2012, 48, 1432-1438.	1.9	4
69	Fourier transform infrared spectroscopic study of nitrogen-doped ultrananocrystalline diamond/hydrogenated amorphous carbon composite films prepared by pulsed laser deposition. Diamond and Related Materials, 2011, 20, 1072-1075.	3.9	13
70	Near-Edge X-ray Absorption Fine-Structure Spectroscopic Study on Nitrogen-Doped Ultrananocrystalline Diamond/Hydrogenated Amorphous Carbon Composite Films Prepared by Pulsed Laser Deposition. Japanese Journal of Applied Physics, 2011, 50, 08JD05.	1.5	3
71	Temperature-Dependent Current-Induced Magnetization Switching in Fe ₃ Si/FeSi ₂ /Fe ₃ Si Trilayered Films. Japanese Journal of Applied Physics, 2011, 50, 08JD06.	1.5	3
72	Fabrication of n-type β-FeSi <inf>2</inf> /p-type Si heterojunctions by pulsed laser deposition and their application to NIR photodiodes. , 2010, , .		0

#	Article	IF	CITATIONS
73	Structural and Physical Characteristics of Ultrananocrystalline Diamond/Hydrogenated Amorphous Carbon Composite Films Deposited Using a Coaxial Arc Plasma Gun. Japanese Journal of Applied Physics, 2010, 49, 015503.	1.5	44
74	Formation of Ultrananocrystalline Diamond/Amorphous Carbon Composite Films in Vacuum Using Coaxial Arc Plasma Gun. Japanese Journal of Applied Physics, 2010, 49, 125503.	1.5	41
75	Nitrogen-Doped Ultrananocrystalline Diamond/Hydrogenated Amorphous Carbon Composite Films Prepared by Pulsed Laser Deposition. Applied Physics Express, 2010, 3, 115102.	2.4	46
76	Optical emission spectroscopy of deposition process of ultrananocrystalline diamond/hydrogenated amorphous carbon composite films by using a coaxial arc plasma gun. Diamond and Related Materials, 2010, 19, 899-903.	3.9	16
77	X-ray photoemission spectroscopic study of ultrananocrystalline diamond/hydrogenated amorphous carbon composite films prepared by pulsed laser deposition. Diamond and Related Materials, 2010, 19, 911-913.	3.9	22
78	X-ray photoemission spectroscopy of nitrogen-doped UNCD/a-C:H films prepared by pulsed laser deposition. Diamond and Related Materials, 2010, 19, 510-513.	3.9	35
79	n-Type Nanocrystalline-\$hbox{FeSi}_{2} /p-Type Si Heterojunction Photodiodes Prepared at Room Temperature. IEEE Electron Device Letters, 2010, 31, 1428-1430.	3.9	16
80	Near-Edge X-ray Absorption Fine-Structure, X-ray Photoemission, and Fourier Transform Infrared Spectroscopies of Ultrananocrystalline Diamond/Hydrogenated Amorphous Carbon Composite Films. Japanese Journal of Applied Physics, 2009, 48, 020222.	1.5	55
81	Time-Resolved Observation of Deposition Process of Ultrananocrystalline Diamond/Hydrogenated Amorphous Carbon Composite Films in Pulsed Laser Deposition. Journal of Nanomaterials, 2009, 2009, 1-6.	2.7	15
82	Characterization of near-infrared n-type β-FeSi2/p-type Si heterojunction photodiodes at room temperature. Applied Physics Letters, 2009, 94, 222113.	3.3	63
83	n -type β-FeSi2/intrinsic-Si/p-type Si heterojunction photodiodes for near-infrared light detection at room temperature. Applied Physics Letters, 2009, 95, .	3.3	41
84	Effect of annealing for CuInS ₂ thin films prepared from Cuâ€rich ternary compound. Physica Status Solidi C: Current Topics in Solid State Physics, 2009, 6, 1030-1033.	0.8	15
85	Near-Edge X-Ray Absorption Fine Structure of Ultrananocrystalline Diamond/Hydrogenated Amorphous Carbon Films Prepared by Pulsed Laser Deposition. Journal of Nanomaterials, 2009, 2009, 1-5.	2.7	38
86	Preparation of KTiOPO4 thin films on different substrates by pulsed laser deposition. International Journal of Advanced Manufacturing Technology, 2008, 38, 600-604.	3.0	6
87	Optical properties of ultrananocrystalline diamond/amorphous carbon composite films prepared by pulsed laser deposition. Diamond and Related Materials, 2008, 17, 1199-1202.	3.9	16
88	Photovoltaic properties of n-Type nanocrystalline-FeSi2/intrinsic-Si/p-Type Si heterojunctions fabricated by facing-targets DC sputtering. Optoelectronic and Microelectronic Materials and Devices (COMMAD), Conference on, 2008, , .	0.0	3
89	Electrical and Photovoltaic Properties of n-Type Nanocrystalline-FeSi ₂ /p-Type Si Heterojunctions Prepared by Facing-Targets Direct-Current Sputtering at Room Temperature. Japanese Journal of Applied Physics, 2008, 47, 5420.	1.5	41
90	Spectral Absorption Properties of Ultrananocrystalline Diamond/Amorphous Carbon Composite Thin Films Prepared by Pulsed Laser Deposition. Japanese Journal of Applied Physics, 2007, 46, L936-L938.	1.5	56

Τςυγοςηι Υοςηιτακε

#	Article	IF	CITATIONS
91	Epitaxy in Fe ₃ Si/FeSi ₂ Superlattices Prepared by Facing Target Direct-Current Sputtering at Room Tempertaure. Japanese Journal of Applied Physics, 2007, 46, 7846.	1.5	16
92	Ultrananocrystalline diamond prepared by pulsed laser deposition. Diamond and Related Materials, 2006, 15, 649-653.	3.9	19
93	Consideration of Growth Mechanism of Diamond Thin Films by Pulsed Laser Deposition. IEEJ Transactions on Fundamentals and Materials, 2003, 123, 939-944.	0.2	0
94	THE ROLES OF AMBIENT OXYGEN AND SUBSTRATE TEMPERATURE ON GROWTH OF DIAMOND THIN FILMS BY PULSED LASER DEPOSITION. International Journal of Modern Physics B, 2002, 16, 825-829.	2.0	3
95	Diode Parameters of Mesa Structural n-Type Nanocrystalline FeSi ₂ /p-Type Si Heterojunctions Prepared by Lift-Off Photolithography. Advanced Materials Research, 0, 1103, 91-96.	0.3	0
96	Ultrananocrystalline Diamond/Amorphous Carbon Composite Films Prepared by Laser Ablation of Graphite in Nitrogen and Hydrogen Atmosphere. Advanced Materials Research, 0, 1105, 274-279.	0.3	0
97	Enhanced Interlayer Coupling and Magnetoresistance Ratio in Fe3Si/FeSi2Superlattices. Applied Physics Express, 0, 1, 021302.	2.4	12
98	Impact of Laserâ€Induced Graphitization on Diamond Schottky Barrier Diodes. Physica Status Solidi (A) Applications and Materials Science, 0, , .	1.8	1